(article starts on next page)

Applicability of thermal energy storage in future low-temperature district heating systems – Case study using multi-scenario analysis

Yichi Zhang [*], Pär Johansson, Angela Sasic Kalagasidis

Department of Architecture and Civil Engineering, Division of Building Technology, Chalmers University of Technology, Gothenburg 412 96, Sweden

A R T I C L E   I N F O

A B S T R A C T

With the flexibilities added from thermal energy storage (TES) technologies, low temperature district heating (LTDH) system can coordinate the heat and electricity sectors in a cost-effective manner. Such combinations have therefore become an important step to achieve a 100% renewable energy system. Despite the importance of TES has been demonstrated in previous studies, giving drastic changes compared to the current systems, the practical applicability of TES in the LTDH systems remains unknown. Furthermore, the proposed benefits of TES might deviate from the expectations considering the development of future characteristics, such as the low temperature levels and small space-heating demand. This study investigates the performances and benefits of four typical short-term TES technologies, including the use of central water tank (CWT), district heating network inertia, domestic hot water tank (DHWT), and building thermal mass, based on a case LTDH system in Roskilde, Denmark. Techno-economic analysis is conducted on a variety of scenarios, based on future changes in operation of the heat sources to the end-users. An integrated model is also developed to simulate the operation dynamics of the district heating system with regards to optimizing the use of the TES units. This study provides a performance map of the TES technologies in accordance with the transitions from current to future LTDH systems, indicating the relationships between the system characteristics and optimal TES applications. The CWT is found to be most preferable for integrating the variable renewable energy due to its ability to store heat for long periods. In the end-use side, with the improved building performances and reduced space heating demand in the future, there is less potential for the use of building inertia. In contrary, the benefit of the DHWT, which mainly comes from the reduction of bypass loss during the non-space-heating period, is increased in the future. Furthermore, raising the network temperatures for active storage is found to be infeasible under all future LTDH scenarios because this measure significantly influences the heat source efficiency.

1. Introduction

The target of a 100% renewable energy system brings drastic challenges for the whole society [1]. With the increasing share of intermittent variable renewable energy (VRE) suppliers, the whole energy systems including the transportation networks and consumers must be re-designed and planned to efficiently utilize the VRE sources. At the same time, the secured energy supplies and acceptable economic expenditures need to be maintained. Solutions to accommodate this balance are studied and aggregated as various pathways towards the future sustainable energy system [2]. It is acknowledged that the integrated design of energy conversions and management between energy subsectors are becoming increasingly important for achievable and affordable strategies.

Currently, the heating sector accounts for 50% of Europe's final energy consumption [3] and is expected to remain so for the forecasted future. Among the solutions to decarbonize the heating sector and increase the renewable energy integration, the concept of the future low temperature district heating (LTDH) is discussed in several studies [4–6]. A low temperature on the circulating water in combination with low heating demands in buildings can enable key benefits including better utilization of low-temperature waste heat and integration of renewable energy sources, as well as lower losses in transportation networks. Furthermore, the heating sector of the LTDH system can be coordinated with the electricity and transportation sectors. Together they can form a smart energy system and enable an optimal transition towards the future 100% renewable energy system [2,7].

In order to achieve such synergies between sectors, thermal energy storage (TES) technologies are widely studied since they can offer

---

* Corresponding author.
  E-mail address: yichi@chalmers.se (Y. Zhang).

Nomenclature

Abbreviations

BTM	Building thermal mass
CHP	Combined heat and power
CWT	Central water tank
DH	District heating
DHNI	District heating network inertia
DHW	Domestic hot water
DHWT	Domestic hot water tank
IWH	Industrial waste heat
LTDH	Low temperature district heating
MILP	Mixed-Integer Linear Programming
SEK	Swedish Krona
SFH	Single-family house
SH	Space heating
TES	Thermal energy storage
VRE	Variable renewable energy

Symbols

A	Area (m^2)
$Cost$	Cost (SEK)
C	Heat capacity (kWh/K)
D	Pipe diameter (m)
F	Cross-sectoral area (m^2)
G	Flowrate (kg/s)
K	Heat transfer coefficient (W/K)
L	Length (m)
λ	Thermal conductivity (W/m·K)

P	Pressure (kPa)
Pr	Operation cost (SEK/kWh)
$\dot{Q}$	Power (W)
SOC	State-of-charge (kWh)
u	Flow velocity (m/s)
A	Incidence matrix of DHN
B	Route matrix
G	Flowrate vector for all branches
ΔH	Pressure drop vector
T_{out}	Outflow temperature vector
R_B	Heat capacity matrix
T_N	Node temperature vector
$\dot{Q}_N$	Energy exchange vector

Subscripts

B	Branch
ch	charge
dch	discharge
demand	Total heating demand
e	Environment
HS	Heat source
i	Inflow
in	indoor
$loss$	heat loss
o	Outflow
out	Outdoor
τ	Time step
x	Coordinates

flexibilities in matching the energy supply and demand on various time scales [8]. Combined with CHP plants and power-to-heat technologies such as heat pumps, TES technologies can increase the VRE integration and reduce the operational cost in existing systems [9,10] and future smart energy systems [11–14]. Common to these studies is a top-down approach where analyses are performed for an entire energy system of a country, e.g. Denmark [12], or a region like Europe [15], without detailing the sublevel systems. Thus, only cumulative storage capacities and costs of TES technologies are addressed. Compared to pathways that only consider electrical storage technologies, the smart energy system pathway with TES technologies can be achieved with significantly lower investments [11].

Despite the importance of TES and future LTDH systems imposed by previous top-down studies [4–6,11–15], relatively less attention has been put on how different TES technologies are adapted and performed in LTDH systems. In a recent review summarizing the applications of TES technologies in district heating and cooling systems [8], the majority of examples refer to the TES applications in the current middle and high temperature district heating (DH) systems. It is, however, worth noting some important changes in the future LTDH systems. Because of lower system temperatures, the heat source efficiency will be more sensitive to temperature changes. Furthermore, the networks and substations are to be re-designed to maintain the return water temperature and avoid bypass heat loses. Meanwhile, space-heating demand and heating periods will be reduced due to better energy efficiency of the future buildings. Considering the above-mentioned changes in the LTDH system, i.e. in the heat sources, networks and end-users, whether the planned TES technologies will perform as intended in the future LTDH systems still remains as an unresolved question.

From the perspective of bottom-level TES applications details in LTDH systems, as the storage temperature difference becomes smaller, the use of sensible active storage units becomes less profitable [16]. Since the system efficiency is more sensitive to temperature levels, the

current plausible storage technologies that have influence on the network working temperatures, such as the use of the district heating network inertia (DHNI) and domestic hot water tank (DHWT), might lose attractiveness in the future. Indeed, the applicability of current TES technologies needs to be well examined.

While both seasonal and short-term storage units are in focus, the latter is a common choice to deal with diurnal variations caused by the intermittent nature of VRE. These variations have strong influence on the marginal operation costs and performances of the DH systems [16]. Thus, the short-term storage units are chosen as study objects. Reviews about the applications of short-term TES units can be found in a series of previous studies [8,17,18], with focuses on the overall technology development [8], the storage potentials of BTM and DHNI [17], and the connections with the electrical grid [18]. However, as in the top-down studies mentioned above, most application studies are restricted to traditional middle and high temperature DH systems. The applicability of short-term TES units in the future LTDH systems remains unknown, which becomes the focus of this study. Detailed explanations of the advantages and challenges for short-term TES technologies in the future are further provided in the Section 2.1, based on the literature review of current studies.

As for the top-level planning of the TES and energy systems, most studies are still taking the current available TES technologies into account, without considering their technical details and applicability in the future. In [11], the potential of DHNI is evaluated based on a fixed temperature increase of 10 K in the network, which is not appropriate according to aforementioned reasons. Similar method is also applied in [19] to evaluate the DHNI in Chinese DH systems. Limitations also exist for evaluating the storage potential of building thermal mass (BTM) [19], since the practical storage capacity is reduced as the heating demand becomes lower in LTDH system. Without the knowledge about operational conditions of TES technologies in the future, there are risks for the exaggerated or underestimated potentials of the TES, which

further influences the energy balance and overall planning of the smart energy systems. The proposed pathways towards the 100% renewable energy target might deviate from the reality. Hence, to prevent biased conclusions for the future energy systems, the technology development and planning of TES shall be in high accordance with the changes in the future LTDH systems.

Considering the knowledge gap illustrated above, this study aims to evaluate how the current TES technologies can be adapted to the changes in the future LTDH systems. Techno-economic analysis and comparisons of four typical short-term TES technologies were performed on a variety of scenarios, which are representatives of the main characteristics of the current and future DH systems. The changes of the DH systems in the source side, substations, and the end-use buildings are considered in the scenarios. The bottom-up analysis is based on an integrated dynamic model for the DH system developed in this study, which can optimize the design and operation of TES units. The model also has enough technical details to depict the characteristics and challenges of TES technologies in LTDH systems. From the results of this study, the optimal design and operation of TES units according to specific future system characteristics are derived. The study provides a clearer understanding about the possible roles of TES technologies in the transition towards the future smart and renewable energy systems.

This paper is organized as follows: Section 2 introduces the background knowledge, including the characteristics and changes of the LTDH systems, and the associated challenges imposed on current TES technologies. Section 3 explains the modelling methodologies and case study. Section 4 describes the investigated scenarios. The results of the multi-scenarios analysis are presented in Section 5. Based on the results, the discussions on the future applications of TES technologies are provided in Section 6.

2. TES technologies and LTDH designs

The concepts and characteristics of LTDH are introduced in Section 2.1, as knowledge basis for the investigations in this study. From the perspective of the future LTDH, an overview of the advantages and challenges with different short-term sensible TES technologies, which are the central water tank (CWT), district heating network inertia (DHNI), building thermal mass (BTM), and distributed domestic hot water tank (DHWT), are explained in the Section 2.2.

2.1. LTDH characteristics

The concepts and main characteristics of LTDH systems are summarized in several studies [4–6]. On the source side, due to the reduction of return water temperatures, the low-grade waste heat from multiple sources can be recovered. Besides, the integration of VRE can be improved through the implementation and smart control of power-to-heat technologies such as heat pumps. It shall be noted that the VRE discussed in this study refers to renewable electric power from intermittent sources, such as wind power and solar power. The relatively stable renewable heat sources such as biomass are not included. In the demand side, an important characteristic is the reduction of space-heating demand in existing buildings and newly built low-energy buildings. Meanwhile, the DHW demand plays more important roles in the total demand. The improved building performances also make the low-temperature heating feasible. Such changes in the demand side

influence not just the heat sources, but also the transportation networks and the use of building thermal inertia.

As pointed out in previous studies [20,21], one important cause for the existing high return water temperatures is the preparation of DHW demand. The instantaneous heat exchanger and domestic hot water tank (DHWT) are two traditional designs that are widely applied in the current DH systems, as shown in Fig. 1. The pipes are filled with hot water to assure an acceptable waiting time, which significantly increase the heat losses and return water temperatures.

In order to maintain the required return water temperature, several solutions were provided by researchers [22–24]. One idea is based on the maximum cooling concept, that the supply water is bypassed to the floor heating pipes in the bathroom or other spaces where additional heating does not create discomfort. Thereby, the return water is cooled down to the required temperature level, as 25 °C in this study. This design is also named "comfortable bathroom" in some studies [22,23]. Thus, the bypass loss is inevitably created by this design. The bypass flowrate shall be carefully designed so the supply water temperature is always within a requirement after a certain degree of temperature drops caused by heat losses on supply lines. This design is applied to the instantaneous heat exchanger and DHWT in this study. Alternatively, the triple-pipes design with a re-circulation pipe can eliminate the bypass heat loss while maintaining the thermal comfort [20], as shown in Fig. 1(c). Due to the required new investment and construction works, the triple-pipes design is suitable for newly built LTDH systems and is therefore considered as one optional scenario for the future LTDH systems. The bypass heat losses and the practical performances associated with the three typical substation types, are evaluated and presented in Section 5.3. There are also other alternative designs, such as the electrical supplementary system [22]. They are currently omitted in this study since they are mostly applicable for ultra-low temperature district heating systems with supply water temperatures lower than 40 °C, which is not the focus of this study. Moreover, in order to avoid legionella growth in LTDH systems, the temperature level inside the DHWT need to be strictly controlled. Otherwise, additional investments for legionella disinfection solutions, such as ultraviolet light, are required [23,25]. These measures have no influence on the performances of the heating systems but will change the economical balances.

2.2. Advantages and challenges of typical short-term TES technologies

The central heat accumulation tank is a storage device that is often installed near the heat sources to balance the heat supply and demand. A common practice is the central water tank (CWT), due to its relatively cheap investment, stable performance, and the possibility of direct connections with the DH system [16,26]. Benefits from installing the CWT are summarized to three points: (1) reduced investment and usage of peak capacity; (2) smoother operation of equipment and reduced running costs; (3) flexible load shifting to utilize non-dispatchable VRE or electricity with lower prices [27]. In Sweden, 104 out of 167 DH systems have installed central TES units [28]. Due to the additional flexibility added to the electricity sector, it is also found that the systems with combined heat and power (CHP) plants have more incentives to install TES units than the systems with industrial waste heat (IWH) as heat sources. However, as indicated above, the energy storage density of CWT will become smaller in the future LTDH systems due to reduced temperature differences. Besides, the inevitable mixture of hot and cold
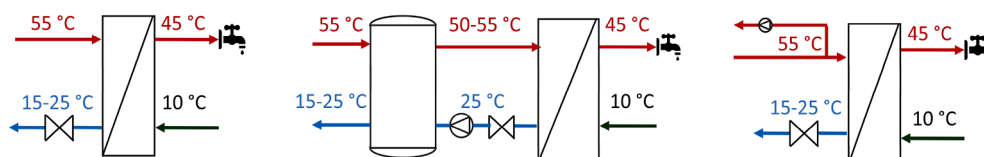

Fig. 1. Three typical substation types for preparing the DHW demand. (a) Instantaneous heat exchanger; (b) domestic hot water tank; (c) triple-pipes.

water inside the tank can increase the return water temperature level and reduce the heat source efficiency [29]. The above-mentioned challenges were only qualitatively indicated in previous studies, while the quantitatively understanding is still lacking.

Distributed DHWT has the similar structure as the CWT and is placed in the consumer side to level out the intermittent DHW demand. Compared to the CWT, additional benefits of reducing the network sizes and related investments can be provided by the demand-side DHWT [30]. However, similar limitations regarding the reduced storage capacity and increased return water temperature also exist. Another important issue associated with the substation design is the bypass heat loss during the low demand period, as described in the previous Section 2.1. Although the improved designs have lower bypass losses and return water temperatures compared to DHWT design, the storage function and related benefits are no longer available. Comparison studies of these designs can be found on the practical substation level [31] and the whole system level [32]. However, most studies only considered the passive buffer benefit of the DHWT, while the active storage benefit is often neglected when comparing different designs. Hence, it is highly relevant to investigate the applicability of alternative substation designs in the future LTDH system.

The use of building thermal mass (BTM) as a storage unit has gained increasing attentions in recent years [17]. Compared to other active storage options, the major advantage of the BTM is the simpler system design and less investment [33]. Thus, the applications of BTM in DH systems were discussed in a variety of studies [34–36]. It is pointed out that the available storage capacity is mostly influenced by the allowed thermal comfort varying range and building types [34]. BTM has also been compared with other TES technologies, such as CWT [37] and distributed heat accumulation tanks [38]. However, the main limitation of BTM is that it can only be utilized during the space heating (SH) period. Since the energy performance of buildings is planned to be continuously improved in the future, with less SH demand and shorter SH period, the storage potential of BTM will be reduced. Moreover, well insulated buildings are prone to overheating. Residents will simply open windows to cool the indoor environment and, thereby, jeopardize the opportunities for storing the heat in the building structures. These limitations of BTM in the future LTDH systems have not been fully covered in previous application studies or energy planning works.

The DH pipelines can be considered as inherent storage units, with the charging and discharging processes achieved by adjusting the temperature levels in the pipelines. Thus, this use of district heating network inertia (DHNI) has the main attractiveness of the less investment, compared to other standalone storage options [17]. Fredriksen and Werner [39] described the limited storage capacity of DHNI and pointed out that larger storage capacity is presented in bigger DH networks, with higher heat demand density. Since the temperature levels are increased, the efficiencies of heat sources are inevitably influenced. Thus, relatively more focuses are paid on the traditional middle and high temperature DH systems in dense population areas, with CHP plants as the main heat source [13,40,41]. In these scenarios, the network supply water temperature is heated up by the extracted steam from the CHP plant and, thus, has little impact on the source efficiency. It is further indicated that the combined use of CHP plant and DHNI can increase the integration of VRE such as wind power, by expanding the regulating ability of CHP plant and reducing the VRE curtailment [41,42]. However, the above conditions that are favourable for the use of DHNI, are no longer effective in future LTDH systems. Firstly, the low temperature sources, such as the heat pump and IWH, are sensitive to both the return and supply water temperature levels. It might be economically and environmentally infeasible to heat up the network for the storage benefit. Secondly, the future heating demand density will be reduced and the LTDH systems will be built with smaller sized pipes, creating less opportunities for the use of DHNI. Besides, the network heat losses are also increased during the charging period. These challenges need to be carefully evaluated when considering the future storage potential of DHNI.

3. Methods

As reported in [6], the small-scale DH systems with small heat demand densities have promising potentials to be upgraded into the LTDH systems. Therefore, a LTDH system in a small residential community in Denmark is chosen for the case study, as introduced in Section 3.1. The techno-economical evaluations of TES technologies are based on numerical simulations and exemplified on the case study. In order to investigate the dynamic performance of the DH system, an integrated system model is developed. Built on the basic input parameters such as the building properties and the network layout, this model can optimize the DH system from design to operation stage. Four main steps of this model and the modelling methodologies are explained in Section 3.2. To investigate dynamic performances of TES units, separate TES models and control strategies are developed to represent the bottom-level technical details. These models are introduced in Section 3.3.

3.1. Case description

The case LTDH system is located in the suburban area of Trekroner in the municipality of Roskilde in Denmark, derived from a previous study [32]. The DH system is supplying heat through a branched network to 165 single-family houses (SFHs), aggregated into 31 substations, as shown in Fig. 2. This case represents a common residential area in Europe with a relatively low heating demand where the benefits of the LTDH, such as the reduction of heat losses and the improved heat source efficiency, can be investigated. The heated floor area is set as 120 m^2 for each SFH and the total heated area for the case LTDH system is 19,800 m^2. The network has a total length of 1.9 km and the pipe sizes are designed by an optimization process, explained in Section 3.2.2. For simplicity reasons, the secondary circulation network between the substation and the end-user SFHs is represented by a 20 m long pipe, which is not shown in the figure. Several heat source options are centred in one plant in the network and their specific characteristics are introduced in Section 4.1 as representative scenarios of the future LTDH systems. The whole year of 2019 is selected as the study period and all external input data, such as the historical weather data and energy prices, are referring to the year 2019. This year was selected since it was the most recent year with a complete set of data at the time of the study (late 2020).
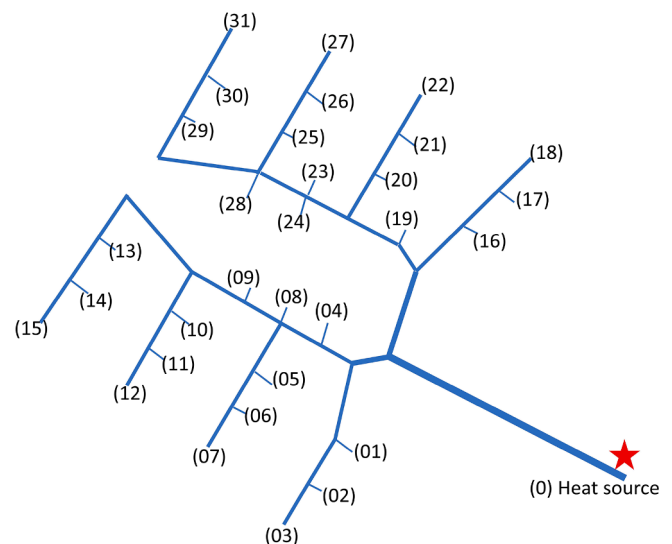

Fig. 2. Network layout of the case DH system, with substations and heat source marked.

3.2. DH system model

The DH system model has four main steps, as shown in Fig. 3. Based on the input building properties and the weather data, the demand profiles for SH and DHW are generated by stochastic modelling method in the first step. Then, considering the network layout and the specific design criterium for working pressures, the pipe dimensions are optimized with the objective to minimize the investment. The designs of the substations and LTDH networks are also included in the second step. For the third step, the temperature and flow dynamics of the network are modelled by the node method [43,44], with considerations of the transport delay and heat losses. Then, the operations of the TES units and the network are optimized in the fourth step. The model also has the capability of adjusting the system design according to the optimization results and, thereby, creates an iterative process between the four main steps. Based on these steps, the multi-scenarios analysis is conducted. The model is developed and performed in MATLAB.

3.2.1. Demand profile

To simplify the computation process, the end-users connected to the same substation are aggregated into only one representative end-user. This simplification is acceptable since the end-users connected to one substation are often the buildings with similar properties and load profiles. The SH demand is calculated by a lumped capacitance building model with five resistances (5R1C), written in Eq. (1), according to EN ISO 13790 [45]. In this representation, each building is considered as one thermal zone with a uniform air temperature. The specific building component properties are explained in Section 4.2 in detail, as design scenarios in this study. The indoor setpoint temperature is 21 °C.

$$C_{eff}\frac{dT_{in}(t)}{dt} = (K_{tr} + K_{vent}) \bullet (T_{out}(t) - T_{in}(t)) + Q_{gain} \tag{1}$$

Where the K_{tr} and K_{vent} are the total conductance for the heat transmission and ventilation part, respectively. T_{out} and T_{in} are the outdoor and indoor air temperature. $\dot{Q}_{gain}$ is the power of the total heat gains. C_{eff} is the lumped heat capacity, comprised of the capacity of indoor air, furniture and interior walls, and the effective thermal mass of the building envelope, according to EN ISO 13790 [45].

In order to consider realistic conditions of DHW usage, the draw-off profile is generated with a time-step of one minute by a stochastic modelling tool called *DHWcalc* [46], built upon statistical methods and realistic draw-off profiles. Four categories of loads are considered in the model. For each category, the actual flowrates are sampled from a normal population with a pre-defined mean value and Gaussian distribution. The probability functions that describe the variations of the load profile during the year, weekdays, and holidays, are also defined. The daily mean DWH load for the case SFHs is randomly chosen within the range of 140 to 160 L/day, which represents the average DHW usage for SFHs in Northern Europe [47].

Based on the above modelling approaches, the theoretical SH demand profile is calculated by the sum of the SH and DHW demand profiles. The practical issues, such as the secondary network heat losses, are illustrated in the following chapters.

3.2.2. System design

The SH part and the DHW part are designed in parallel in the substation, as shown in Fig. 4. To maintain low return water temperature, the SH part uses a heat exchanger with high thermal lengths, as pointed out in [20]. This design is consistent over all substations and all scenarios in this study.

With a requirement of short waiting time, the secondary circulation pipe is often filled with hot water, which causes high circulation heat losses. Compared to the SFH substation, this issue has larger impact in large substations with several end-users, such as the multi-family building substation. As mentioned above, the circulation pipe length is set as 20 m in each substation. Related heat loss for each branch pipeline is calculated according to Eq. (2).

$$\dot{Q}_{B,loss} = K_B * L_B * (T_B - T_{soil}) \tag{2}$$

where K_B is the linear heat loss coefficient. L_B is the pipe length. T_{pipe} and T_{soil} are the water temperature inside the pipe and the surround soil temperature, respectively.

The case system is designed to have a fixed supply water temperature and variable flowrate. The outlet water temperature from the heat source is set as 55 °C and the maximum allowable temperature drop on the primary pipeline due to heat losses is set as 5 °C. The return water temperature is varying between 20 and 30 °C due to the above-mentioned factors. As explained in Section 2.1, the comfortable bathroom design and the alternative triple-pipes design are considered to maintain the return water temperatures.
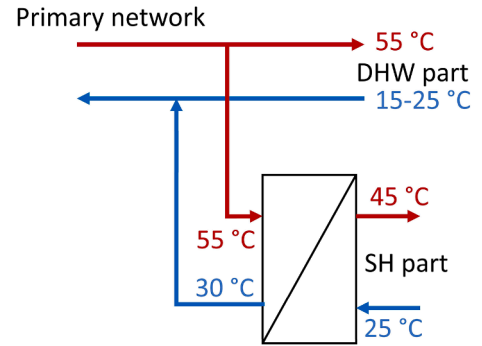

Fig. 4. Substation design for preparing the SH demand.
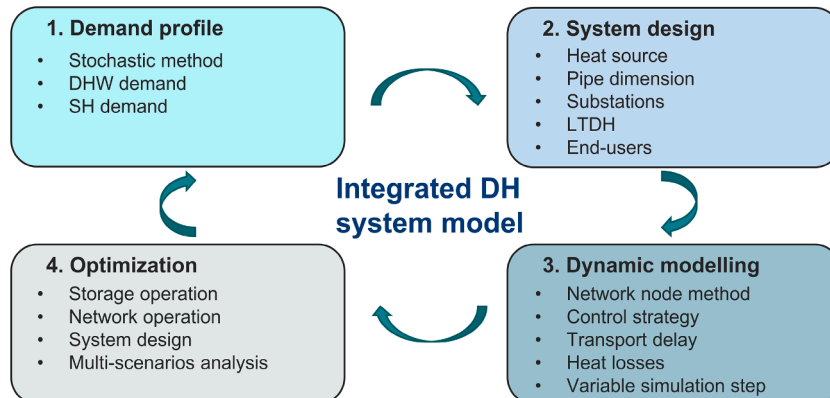

Fig. 3. Schematic of the main steps of the integrated DH system model developed in this study.

After acquiring the theoretical demand profile and network input data, the optimal pipe dimensions are selected by the Mixed-Integer Linear Programming (MILP) process with the objective of minimal investment, written in Eq. (3). Since the heat loss rate mainly depends on the temperature and pipe sizes [32], the optimization target also represents the minimal total heat loss. For each route, the maximum pressure drop limit is set as 6 bar, as is expressed in the constraint in Eq. (4). The pressure drop in the branch pipe is calculated using the Darcy–Weisbach equation for circular pipes due to its simplicity and applicability in a variety of flow conditions.

$$\text{Minimize} \sum_B (C_B * L_B) \tag{3}$$

$$\nabla P_B = f(D_B, G_B, L_B, v, \epsilon) \leq \nabla P_{B,\text{Max}} \tag{4}$$

where C_B refers to the network construction cost of each branch pipeline, determined with the medium cost from several piping companies [48], as shown in Appendix Table A.1. The currency used in this study is Swedish Krona (SEK), which equals to on average 0.095 Euro for the whole year of 2019. D_B and G_B are the diameter and the design flowrate for each branch, respectively. v is the fluid viscosity and ϵ is the pipe absolute roughness height.

3.2.3. Dynamic modelling

Based on step 1 and step 2 in the integrated model, the fixed variables in the LTDH system, such as the network layout, pipe dimensions, building properties and theoretical demand profiles, are specified for following steps. In order to simulate the temperature and flow dynamics of the large DH system, an integrated node, pipe, and energy balance model is applied in this study. The basic principle is that the flow dynamics are firstly calculated by node model and the temperature dynamics and energy exchanges are updated later by the pipe model and energy balance equations.

Based on the Kirchhoff balance laws, the node model was developed in [43,44] and is since then widely applied in dynamic network models [35,40,49]. Therefore, only the general modelling approach is illustrated here, while other modelling details can be found in the cited works. The topology of the network is described by a graph approach. Each pipe is defined as a branch, with an inlet node and an outlet node. The reference flow direction is pre-defined based on the reference velocity in the branched network. The end-use substation is also simplified to a pipe that connects the supply branch and return branch as shown in Fig. 5. The heat exchange through the substation is expressed as $Q_{\text{substation}}$ on the return node. Similar simplification is applied to the heat source. For the chosen case study, with 31 substations and one central heat source plant (see Fig. 2), the network model comprises of 147 branches, 118 nodes, and 31 routes. The incidence matrix, A (118 × 147), is used to express the connections between the nodes and branches. The basic element A_{ij} equals 1 or −1 if the branch j is leaving or entering the node i, respectively. Accordingly, the connections between the routes and branches are expressed by the route matrix, B (31 × 147), where the value 1 or −1 represents a same or inverse flow direction.

For the entire network, the mass balance equation and pressure balance equation can be written in the matrix form in Eqs. (5) and (6).
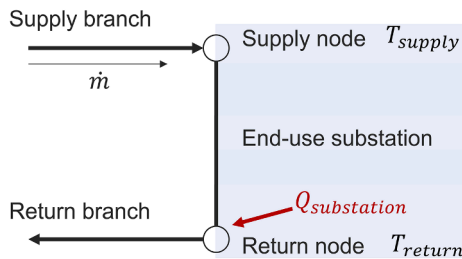
$$AG_B = G_{ext} \tag{5}$$

$$B_f \Delta H = 0 \tag{6}$$

where G_B is the flowrate vector for all branches. G_{ext} is the vector that expresses the mass flowrates leaving or entering the node, possibly caused by the network leakages and supplementary water in practical DH systems. ΔH is the vector that contains the pressure drops for all branches, calculated by the Darcy–Weisbach equation as illustrated in the above section.

In order to simulate the temperature dynamics, the pipe model and energy balance equations are integrated into the network node model. Considering the heat loss and transportation delay, the outlet temperature of the branch pipe at current time step $T_{B,out}(\tau)$, can be expressed as a step response to the temperature difference between the inlet temperature and the environment temperature, written in Eq. (7). A schematic diagram of the pipe model can be found in Fig. 6.

$$T_{B,out}(\tau) = T_{B,in}(\tau - \Delta\tau)e^{\frac{-K_p L_B}{u}} + T_e\left(1 - e^{\frac{-K_p L_B}{u}}\right) \tag{7}$$

where $T_{B,in}$ is the inlet temperature for the branch, which is also the temperature of the previous connecting node. T_e is the environment temperature for calculating the heat losses and can be regarded as soil temperature T_{soil}. $\Delta\tau$ is the transmission delay. K_p is expressed through Eq. (8).

$$K_p = \frac{K_B}{A_{cross}C_p\rho} \tag{8}$$

where K_B is the linear heat loss coefficient and A_{cross} is the Cross-sectoral area of the pipes.

For each node, the inlet energy equals the outlet energy. Thus, the energy balance equation for the network can be written in the matrix form as Eq. (9). With the given flowrate from the node model, Eq. (9) has 118 unknow variables and 118 equations and, thereby, can be solved. Due to the coupling between mass and energy equations, the problem is solved by the iterative algorithm.

$$A_i R_B T_{out} - A_o R_B A_o{}^T T_N = \dot{Q}_N \tag{9}$$

where A_i and A_o are the inflow and outflow matrix, derived from the incidence matrix A to describe the specific connections between the nodes and branches. R_B is a diagonal matrix that contains the heat capacity of branches. T_{out} is the outlet temperature of each branch, expressed by Eq. (7). T_N is a vector that contains the node temperatures at current time step τ and is the unknown variable to be solved in the equation. $\dot{Q}_N$ represents the energy exchange between the node network and the exterior environment. The value could be the heating power in the source side or the substation heating demand, as shown in Fig. 5. As illustrated in the above Section 3.2.2, a fixed supply water temperature control strategy is applied in the case LTDH system. Hence, the Eq. (9) has 117 unknown node temperatures and 1 unknown node input power.

3.2.4. Optimization

Based on the dynamic system model, the practical demand profile and heat source supply profile can be acquired at the reference scenario, where active management is not applied. The system is operated to
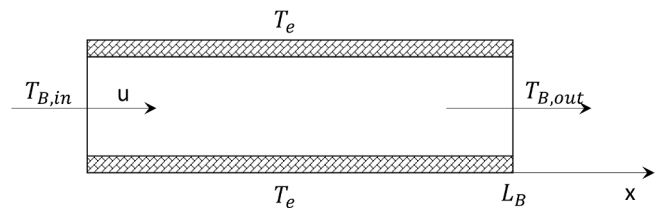

Fig. 5. Schematic diagram of the node model in end-use substations.

Fig. 6. Schematic diagram of the pipe model.

directly fulfil the consumers' demand. However, by utilizing the TES units, additional flexibility to shift the supply and demand profiles is implemented in the system. With a specific target of the lowest system running cost in this study, the objective of step 4 is to find the optimal operation scheme of the TES units, as well as the whole LTDH systems. The proposed model can be further improved to suit other optimization targets. The general optimization approach is explained in this section and the detailed models for the TES units are explained in the following Section 3.3.

Due to the non-linear characteristics of the TES units and the complex DH system, it is hard to find a global optimal result for the non-convex problem that consider the decisions of all TES units. This task becomes even more complicated in the larger system with several distributed TES units. Thus, a combined central optimization and local control strategy is applied, to simplify the optimization process while maintaining realistic characteristics of the control system. The basic idea is shown by the schematic diagram in Fig. 7.

The objective function of the central optimizer is written in Eq. (10). The costs of heat sources are used to represent the overall system cost, while the costs for water circulation pumps and other auxiliary equipment are omitted. As for the source cost, due to the relatively small share of the ramping and start-up cost in the small-scale LTDH system, only the energy cost is considered in this study. However, as indicated in [37], the ramping cost is a non-negligible part in city-scale DH systems with multi heat sources and, thus, has optimization potentials.

$$\min Cost_{HS} = \sum_\tau (Pr_{HS,\tau} * \dot{Q}_{HS,\tau}) \tag{10}$$

where $\dot{Q}_{HS,\tau}$ and $Cost_{HS}$ are the total heat supply and cost of the heat source. $Pr_{HS,\tau}$ is the operation price of the heat source at time step τ, calculated according to the efficiency and input energy cost. The specific values for the investigated heat sources are presented in detail in Section 4.1.

For each time step τ, the heat balance equation is expressed in Eq. (11). $\dot{Q}_{TES,ch,\tau}$ and $\dot{Q}_{TES,dch,\tau}$ represent the charging and discharging power of the TES unit at time step τ, respectively. $\dot{Q}_{demand,\tau}$ is the total heating demand.

$$\dot{Q}_{HS,\tau} + \dot{Q}_{TES,dch,\tau} - \dot{Q}_{TES,ch,\tau} \geq \dot{Q}_{demand,\tau} \tag{11}$$

At time step τ, the state-of-charge of the TES unit, $SOC_{TES,\tau}$, is updated based on the state of the last time step ($\tau - 1$), the energy exchange, and the storage heat losses $Q_{TES,loss,\tau}$, as shown in Eq. (12).

$$SOC_{TES,\tau} = SOC_{TES,\tau-1} + \dot{Q}_{TES,dch,\tau} - \dot{Q}_{TES,ch,\tau} - \dot{Q}_{TES,loss,\tau} \tag{12}$$

For TES units, there are constraints for the state-of-charge and powers, expressed in Eqs. (13)–(15). These general equations are applicable for all investigated TES units in this study.

$$SOC_{TES,min} \leq SOC_{TES,\tau} \leq SOC_{TES,max} \tag{13}$$

$$0 \leq \dot{Q}_{TES,dch,\tau} \leq \dot{Q}_{TES,dch,max} \tag{14}$$

$$0 \leq \dot{Q}_{TES,ch,\tau} \leq \dot{Q}_{TES,ch,max} \tag{15}$$

To assure a reasonable use of the storage capacity, the state-of-charge of the TES unit shall return to the state at the starting point after a complete optimization cycle. In this study, the optimization time step is one hour, and the dynamic calculation step is one minute, in accordance with the demand profile. The length of an optimization cycle is set as 5 days, considering the accuracy of forecast and the control complexity.

3.3. Thermal energy storage models

This study focuses on how the specific TES technology is adapted to the future changes, thus, the combined use of several TES units integrated within one system is currently not considered. Four typical short-term TES technologies, which are the CWT, DHNI, DHWT and BTM, are investigated separately. Together with the reference (REF) system with no TES unit, the five systems were individually simulated in all scenarios.

Although the simplified plug-flow model has been generally introduced for central optimization, the specific constraints related to each TES designs have also been considered and presented in this section together with the detailed TES models. Table 1 summarizes the design parameters of the TES units. To make the evaluations fair, the volume of the CWT and the total volume of the distributed DHWTs are set the same. However, since the DHWT is placed in the consumer side with a 10 °C inlet cold water, it has a higher storage temperature difference and a larger designed storage capacity compared to the CWT. The design parameters of the DHNI and the BTM are derived from the network structures and the building properties, illustrated in the following sections.

3.3.1. Central water tank

The CWT has parallel connection to the heat source. A one-dimensional vertically stratified WT model with 20 layers was used, which has been commonly applied in several WT optimization studies [50,51]. For each layer, heat and mass transfer by convection and conduction are considered, as explained in Eq. (16).

$$\rho VC_p \frac{\partial T}{\partial t} = A_{cross}\lambda \frac{\partial^2 T}{\partial x^2} - G\rho C_p \frac{\partial T}{\partial x} - K_{cwt,loss}A_{ext}(T - T_e) \tag{16}$$

where x is the vertical coordinate. Water mass flowrate G is based on a control signal of the CWT, which is consistent for all nodes. $K_{cwt,loss}$ is the heat loss factor of the CWT, which is assumed to be 0.3 (W/m^2·K) [52]. A_{cross} and A_{ext} are the cross-sectoral and exterior surface area of

Table 1
Design parameters of the TES units.

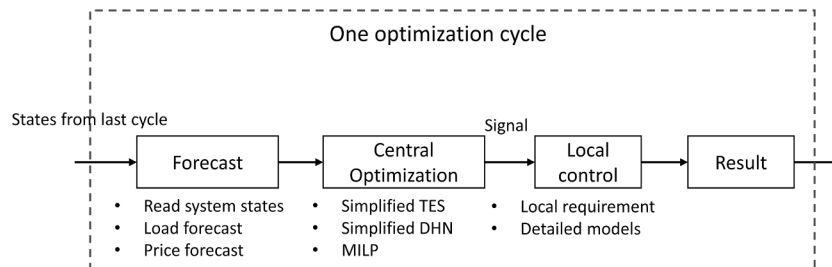| Parameters	CWT	DHNI	DHWT	BTM
Size (m^3)	27.9	2.2	27.9	–
Storage temperature difference (K)	25	10	40	0.5
Storage capacity (kWh)	814	26.1	1302	785
Percent in average daily load (%)	14.3%	0.5%	23.0%	13.8%

Fig. 7. Schematic diagram of the combined central optimization and local control strategy.

each layer, respectively. For simplicity, the heat losses are calculated by the temperature difference between the hot water and surrounding environment.

With the temperature sensors installed in the CWT, the temperature constraints are included in the control system to assure the thermal comfort and system performance. During the discharging period, the outlet water temperature from the CWT will gradually decrease due to inevitable mixtures of hot and cold water inside the tank. The lower limit for outlet water temperature from the top of the CWT is set as 53 °C, which is 2 °C lower than the design supply water temperature. During the charging period, the upper limit for the outlet water temperature from the bottom of the CWT is set as 35 °C, to keep an efficient operation of the heat sources. Hence, the state-of-charge constraints are revised based on the above limits.

3.3.2. Domestic hot water tank

The modelling approach for the DHWT is the same as the CWT. However, the DHWT only has 10 layers to suit the practical stratifications in small-sized water tank [50]. The sizes of the DHWTs in the substations are designed according to the criteria of a 150 L tank for each SFH. Hence, the total volume of the DHWTs is 27.9 m^3, which is also the design volume of the CWT. Unlike the CWT that has an extensive thermal insulation to reduce the heat loss factor to 0.3 W/(m^2·K), the DHWT has less insulation due to a relatively high investment cost per volume and the extra space the insulation layer takes. Thus, the heat loss factor of the DHWT is set as 1 W/(m^2·K) according to a previous field measurement study [53]. The maximum primary flowrate for a typical DHWT of 0.9 m^3 during the charging period is set as 0.18 m^3/h.

To guarantee the comfortable and safe DHW supply, a deterministic local controller is applied for the DHWT, as shown in Fig. 8. The controller reads the central optimization signal and decides the practical charging power P, based on the monitored temperatures at the top and the bottom of the tank. It shall be noted that, to avoid frequent charging operations, the temperature T_{top} is monitored at the second top layer. When the T_{top} is lower than 50 °C, which means the storage capacity is low, the charging power is set to maximum to assure the required supply water temperature in following operations. Otherwise, if the T_{top} is higher than 51 °C, the charging power is controlled according to the central optimal signal. During the idle conditions, the charging power remains the same as the previous time step. Similar as the CWT, a limit of 35 °C is set for the bottom-level water temperature to maintain the required low return water temperature.
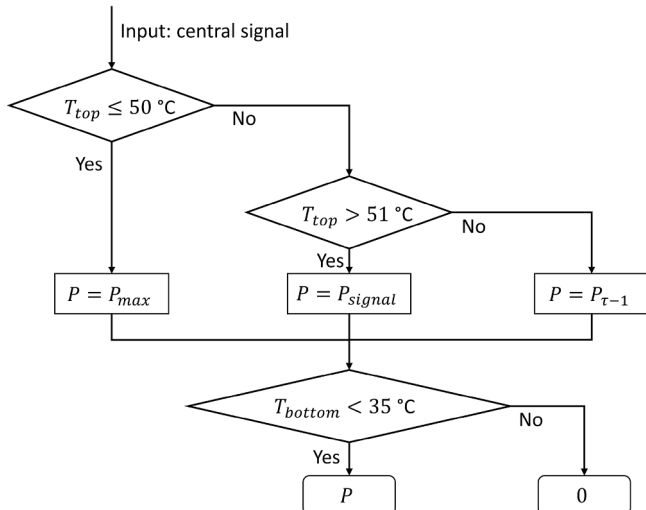
3.3.3. Building thermal mass and district heating network inertia

As illustrated in Section 3.2.1, the SH demand is calculated by a lumped capacity building model. The available storage capacity of the BTM is decided by the effective (interior) heat capacity of the building and the temperature deviations from the setpoint. Results from a previous field measurement of BTM in Gothenburg, Sweden [34], showed that the temperature deviation of 0.5 K above the setpoint temperature is acceptable and thus used in this study. The impact of this constrain is further analysed and discussed in Section 5.5, by modelling three extra temperature deviation scenarios for the BTM. Indeed, by considering only the temperature changes above the setpoint, the systems are using more energy than the reference scenario. Otherwise, if temperature changes below the setpoint are allowed, the systems tend to reduce the thermal comfort levels for lower energy consumption. This belongs to an energy-saving measure but not an active load shifting measure of the storage unit.

As for the use of DHNI as storage unit, an active temperature increase of 10 K in the transportation pipes is assumed in this study. This assumption is set the same as in previous studies (e.g. [11]), to make results comparable. However, the return water temperatures are kept the same as is illustrated in the above strategies, to avoid negative impact on the source efficiency. Thus, only half of the network storage capacity can be utilized. Based on the network layout and the optimized pipe dimensions from the model function 2, the total volume of the water in the supply transportation pipes is calculated as 2.2 m^3. Hence, the theoretical storage capacity is 26.1 kWh, which is relatively small compared to the other three TES options. Indeed, as pointed out in previous studies (e.g. [39]), the network storage capacity is larger in bigger DH networks. The state-of-charge of DHNI at time step τ, $SOC_{DHNI,\tau}$, is calculated according to the difference between the network temperature and the reference temperature. To avoid frequent changes in the network temperature, the minimum charging period is set as 5 h, which is also in accordance with the charging period of other TES units. Then, the maximum charging power is also defined.

3.4. Analysis indicators

In order to compare the storage performances of different TES units, the number of full-load discharge cycles is defined in Eq. (17) in accordance with [37].

$$Full-load\ discharge\ cycles = \frac{\sum_{\tau}\dot{Q}_{TES,dch,\tau}}{SOC_{TES,design}} \tag{17}$$

During the entire year of 2019, the dynamic performances of the reference system without TES options is firstly investigated. Then, the case LTDH systems with different TES technology under different scenarios are modelled and compared. Thus, the cost-saving rate is calculated in this study to evaluate the economic benefits of the TES units, as defined in Eq. (18).

$$Cost-saving\ rate = \frac{Cost_{ref} - Cost_{TES}}{Cost_{ref}} \tag{18}$$

4. Scenarios

With the aim of evaluating the applicability of TES, the performances of the LTDH system were investigated under several scenarios, which represent the possible future changes in the DH system, including the sources, substations, and end-use buildings, as shown in Table 2. The major changes in the substation that this study has considered are the alternative designs to reduce bypass loss, such as the triple-pipes design, which has already been introduced in the Section 2.2. The changes in the heat sources and the end-use buildings are also explained in this section.

Fig. 8. Local control strategy for the DHWT.

Table 2
Summary of the investigated scenarios.

Heat sources	Substations	End-use buildings
Peak scenario	Current design with bypass loss	Current buildings
Variable renewable energy (VRE) scenario	Triple-pipes design	Future low-energy buildings
Industrial waste heat (IWH) scenario		

4.1. Heat sources

As is explained in [4], a key characteristic of the future LTDH system is the ability to recycle heat from low-temperature sources and integrate VRE sources such as solar and wind power. Thus, three typical scenarios of the heat sources are investigated and presented hereafter.

4.1.1. Peak scenario

Two baseload heat pumps and one peak boiler are installed in the modelled LTDH system. Based on the heating power duration curve in the reference scenario, the total heat capacity of the two baseload plants is designed to supply 90% of the heat demand, while the remaining 10% is supplied by the peak boiler. This scenario represents the current DH system where the main incentive for using the TES units comes from the reduced costs due to less usage of peak boilers.

The design parameters of the three heat sources are presented in Table 3. As for the two baseload heat pumps, the COP is calculated by the empirical equation with the condensing temperature and evaporating temperature [54]. The waste-water temperature at the source side is set as a stable value of 15 °C. The thermodynamic efficiency is set as 0.65 and 0.55 for the source 1 and source 2, respectively. Thus, the source heat pump 1 has a higher COP than the source 2. The operation costs of the two heat pumps are the electricity bills, calculated by the hourly variable electricity prices from the NordPool spot market [55]. The average electricity price during 2019 is 1.5 SEK/kWh whereof 33% is the variable part. The reference costs under the average electricity price are also presented in Table 3. As for the peak boiler, considering the practical fuel cost and taxes, a fixed operation cost of 0.75 SEK/kWh$_{heat}$, derived from a previous study in Gothenburg [37], is applied in this study.

4.1.2. Variable renewable energy (VRE) scenario

VRE scenario represents the condition where the TES units are applied to increase the integration of intermittent VRE. In this scenario, 900 m^2 of crystalline solar PV panels are installed in the case system. Each panel has an area of 1.67 m^2 and a nominal system loss of 14% [56]. There are 540 panels installed and the total power generation capacity is 178.2 kW. The hourly power generation profile at the case location is calculated by the Photovoltaic Geographical Information System-interactive (PVGIS) tools [57]. The annual power generation from the PV system is 153.3 MWh, while only 62.1 MWh can be consumed by the reference LTDH system without any TES options. The feed-in price for the residual PV power is set as 0. The heat sources are

set the same as in the peak scenario. Therefore, the optimization objective of the lowest cost is also the objective of the maximum PV integration.

4.1.3. Industrial waste heat (IWH) scenario

In contrary to the above two scenarios where power-to-heat technologies are applied, the IWH scenario uses directly exchanged waste heat from industrial processes. Therefore, the system is not connected to the electricity network and cannot integrate VRE such as solar power. However, as pointed out in several studies [4,7,15], the high efficient utilization of IWH is an important step for a sustainable future, especially in regions where IWH resources are abundant. Another characteristic of the IWH is that, the source efficiency and cost are more sensitive to return water temperature than the heat pumps [58].

In the IWH scenario, the baseload is supplied by two industrial process with a constant temperature of 60 °C, which can heat the network circulation water to 55 °C. The costs for the two sources are set as 0.18 SEK/kWh$_{heat}$ and 0.25 SEK/kWh$_{heat}$, respectively [58]. Due to the requirement of the heat exchanging process, maximum flowrates limits, which are calculated based on the design heating capacity, are also applied for the two sources, as shown in Table 4. The peak boiler is assumed to be the same as the other two scenarios. The design heating capacity is defined based on the average return water temperature of 30 °C. Thus, the reduction of the return water temperature will directly increase the recovered waste heat and reduce the usage of peak boilers.

4.2. End-use heating demand

Another key characteristic of the future LTDH system is the improved energy performance of buildings through building renovations and newly built low-energy buildings. With less SH demand and shorter SH period, there are more variations in the demand profile, induced by the intermittent nature of the DHW demand. Besides, the storage potential of the BTM is also reduced in well-insulated buildings. To investigate the influence of the heating demand change on the TES units, two scenarios that represent the current building stock and the future low-energy building stock, are studied.

The thermal transmittances (U-values) of the building components are presented in Table 5. For simplicity, in all scenarios, the SFHs have the same structures and properties. A constant ventilation rate of 0.5 h^{-1} is assumed in both scenarios. However, heat recovery measures are implemented in the future low-energy buildings to further reduce the ventilation loss. The accumulated SH demand and other key performance indexes are summarized in Table 6.

Based on the integrated DH system models, the reference systems with the current and future building stocks are simulated. A breakdown analysis of the total heat supply in two scenarios is presented in Fig. 9. The network loss refers to the transmission heat loss through the transportation pipes, while the bypass loss refers to the heat loss due to return water temperature requirement, as explained in Section 3.2.2. It can be noticed that as the SH demand decreases, the heat losses and DHW demands become increasingly important. In the future low-energy building stock, the non-space-heating period becomes longer, and a certain flowrate of hot water is required during this period, which increases the bypass loss. In general, the heat losses in two building stocks

Table 3
Design parameters of the heat sources in the peak scenario.

Name	Capacity (kW)	Design COP	Reference cost (SEK/kWh$_{heat}$)	Notation
Baseload source 1	150	4.8	0.31	Waste-water source heat pump
Baseload source 2	200	4.0	0.38	Waste-water source heat pump
Peak source 3	500	–	0.75	Wood pellets heat-only boiler

Table 4
Design parameters of the waste heat sources in the IWH scenario.

Name	Source (°C)	Max flowrate (t/h)	Reference cost (SEK/kWh$_{heat}$)	Design capacity (kW)	Notation
Baseload source 1	60	5.1	0.18	150	Industrial waste heat
Baseload source 2	60	6.8	0.25	200	Industrial waste heat

Table 5
U-values of the building components in the current and low-energy building scenarios.

Elements	U-value (W/m².K)	
	Current	Low-energy
External wall	0.25	0.11
Roof	0.21	0.05
Floor	0.19	0.08
Window	1.2	0.7

Table 6
Performances of the current and low-energy buildings.

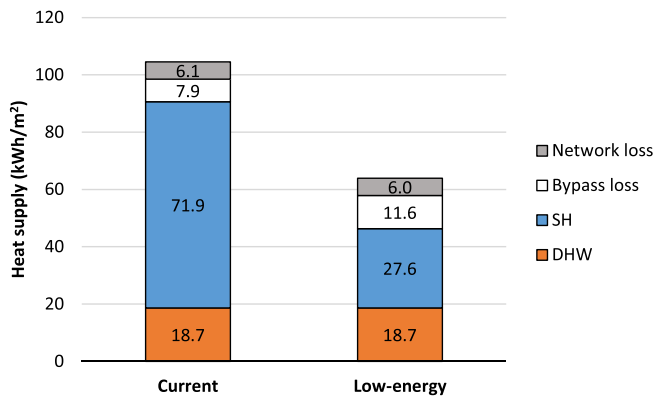| Buildings	Heat loss (W/K)	Internal heat capacity (kWh/K)	Time constant (h)	SH period (h)	Heating demand (kWh/m²)	Heating power (W/m²)
Current	128.4	9.5	74	5715	80.6	28.2
Low-energy	67.3	9.5	141	4159	34.7	14.1

Fig. 9. Annual heat supply per unit heated area for the current and future low-energy building stocks.

are 13% and 28% of the total heat supply, respectively.

5. Results

Based on the methodologies illustrated in the above sections, the scenarios designed in Section 4 were simulated at an annual period and the results were compared. This section first shows the performance differences of TES technologies at the baseline scenario, where current building stocks and the peak heating source scenario are applied. Then, the applicability of TES technologies under the influences of the heating sources, substation designs, and the end-use demand are analysed. Moreover, the sensitivity of the storage potentials from the BTM is further analysed and discussed.

5.1. Peak heat source scenario with the current building stock

In the peak scenario, the objective of the optimization is to reduce the use of peak boiler by shifting the demand to the baseload plants during off-peak periods. An example result of the peak-shaving effect of the CWT under typical winter days between Jan 1st and Jan 5th is shown in Fig. 10. Since the total heat capacity of the two baseload plants is 350 kW, the peak load above this limit, which is normally caused by the intermittent DHW demand in the morning and in the evening, is shifted to the baseloads (see the heating load differences at the 20th hour in Fig. 10). Yet, there is still a few hours of high-peak demand which cannot be shifted due to the limited storage capacity of the CWT. The main principle for other TES units is the same as the CWT but the practical performances and delivered benefits are quite different, which are presented in Table 7.

In the REF system, the peak load is 169 MWh, which is 8.2% of the total DH supply. As for the storage performances, the BTM has the lowest full-load discharge cycles because it is only used during the SH period. The CWT has the highest storage efficiency while the DHNI has the lowest, due to the network losses. The CWT also has the largest peak load reduction and thus has an annual cost-saving rate of 2%. Although the peak load reduction by the DHWT is smaller than the CWT and the BTM, the saved operation cost is the highest among the four TES units. This can be explained by the heat losses in the whole system, as shown in Fig. 11. Compared to the REF system, an extra TES loss is added in the four systems with TES units. The TES loss in the DHNI system is transformed to the increased network loss. Although the DHWT system has the largest TES loss, it can significantly reduce the bypass loss and thus has approximately a 4 kWh/m² lower heat loss compared to the other investigated systems. During the non-space-heating period, the original bypass heat loss as required to maintain the low return water temperature is collected and used in the DHWT. However, the return water temperature might be slightly increased due to inevitable mixing inside the tank. This issue is further explained in the Section 5.2.

For the system using the DHNI as storage media, the total operation cost is even higher than the reference system without any TES options.
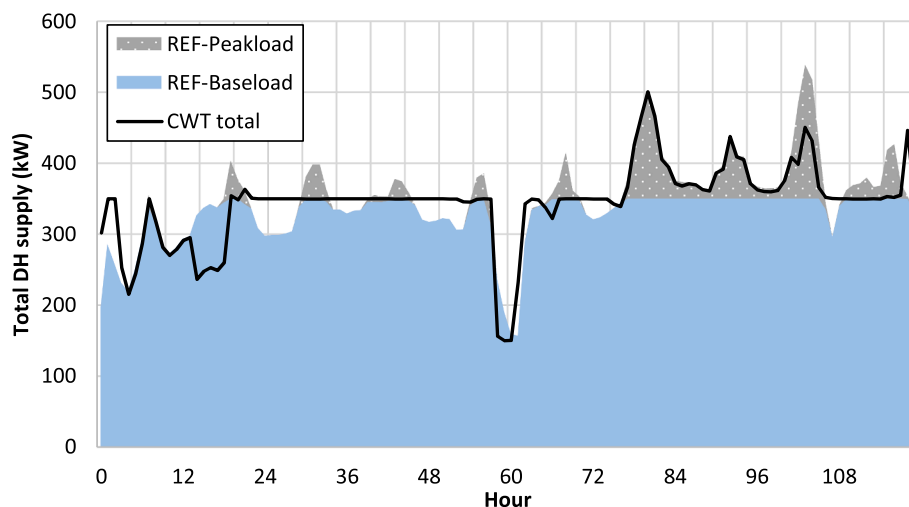

Fig. 10. Total heat supply of the REF system and the CWT system between Jan 1st and Jan 5th.

Table 7
Storage performances and annual cost-savings of the TES units.

Scenarios	Charge (kWh)	Discharge (kWh)	Efficiency (%)	Cycles (n)	Peak load (kWh)	Cost (SEK)	Cost saving rate (%)
REF	–	–	–	–	169,005	775,050	–
CWT	178,805	174,150	97%	134	−33,018	−15,374	1.98%
BTM	68,590	56,941	83%	52	−20,329	−8256	1.07%
DHWT	363,172	317,971	88%	244	−8066	−18,835	2.43%
DHNI	11,565	7052	61%	267	−2687	12,171	−1.57%
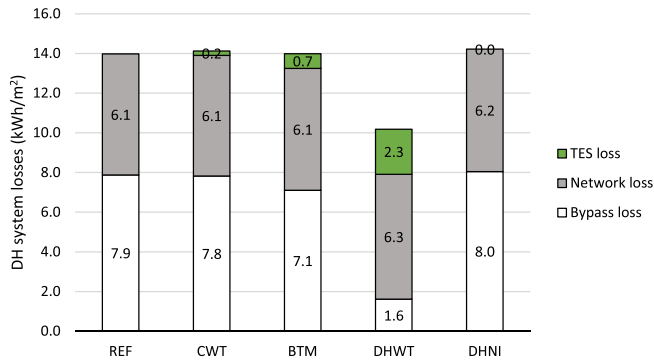
Fig. 11. Breakdown of annual heat losses in the case system with different TES units.

This is mainly due to the reduced source efficiency by raising the network supply water temperature, but also due to the increased network transmission losses. The annual average COP of the two heat pumps in the DHNI system are 4.8 and 4.0, while the average COP in the REF system are 4.9 and 4.1. Besides, as shown in Fig. 10, the use of DHNI further increases the network loss and bypass loss due to the higher supply water temperature. Considering the relatively small storage capacity and small peak-shaving benefit, it is not economically feasible to use the DHNI in the case LTDH system. However, as indicated in the introduction, the DHNI has possible benefits in large, traditional DH system. The applicability of this technology needs to be further investigated in detail.

5.2. The influence of heat sources

The performances of TES technologies under the VRE scenario and the IWH scenario, as explained in Section 4.1, are compared in this Section. In the VRE scenario, the annual VRE integration rate and the cost-saving rate are presented in Fig. 12. The CWT has the largest potential for integrating VRE and thus has the largest cost-saving rate of 7.7%. Compared to the REF system, an additional 26 MWh of VRE is consumed by the CWT system. Although the DHWT is designed to have a larger storage capacity than the CWT, as presented in Table 1, its actual capacity to integrate the excessive VRE is not proportionally larger. This
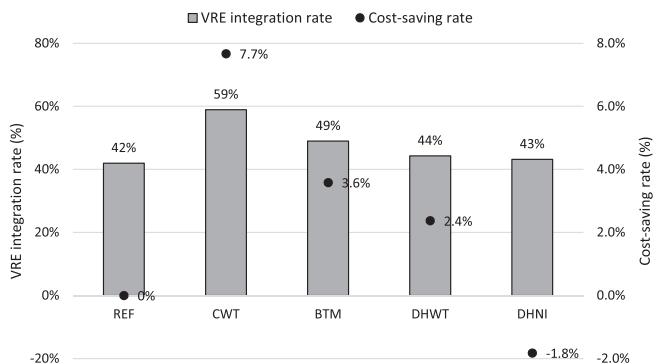
Fig. 12. Annual cost-saving rate and VRE integration rate in VRE scenario.

can be explained by the larger heat losses and temperature restrictions from the DHWT when charged in idle state for a longer period.

The number of occasions when the state-of-charges of the TES units are higher than 70% of their design values, classified by the number of consecutive hours that each occasion has, are shown in Fig. 13. Due to the smaller heat loss and the control simplicity at the source side, the CWT can store energy for a longer period than the other technologies. There are 134 occasions where the CWT is used to store heat for more than 10 h. In contrary, the DHWT is mostly used for less than 10 h. The TES with a longer storage period can better deal with the variations in the VRE generation caused by weather conditions. The average consecutive hours for the CWT, BTM, DHWT, and DHNI are 10 h, 5.9 h, 5.8 h, and 3.1 h, respectively. Another reason for the relatively low cost-saving rate for the DHWT is that the previous benefit from the reduced bypass loss is less significant during the Summer season when VRE productions and cheap electricity prices are available.

As for the IWH scenario, the efficiency of IWH resources is more sensitive to the return water temperature compared to the heat pumps. The daily average return water temperatures of the REF, CWT, and DHWT systems are shown in Fig. 14. To make the expression clear, the temperatures of the BTM and DHNI systems are not plotted. Due to strict bypass design and control, the REF system has the lowest return water temperature among the investigated systems. The return water temperatures are gradually increased from Summer to Winter, under the influence of the SH demand. The use of CWT slightly increases the temperature since a part of the return water is inevitably mixed with hot water inside the tank. However, due to the control complexities for distributed small tanks, the DHWT system has the highest return water temperature, which is about 2.8 °C higher than the average temperature of the REF system. This phenomenon is more prominent during non-space-heating period. The instantaneous DHW demand is transformed into regularly controlled demand in hot water tanks. From this process, the bypass loss is significantly reduced but the return water temperature is also increased. This characteristic of the DHWT system is also reported in [20,30]. To overcome this problem, stricter controls of the return water temperatures, such as the constraints in Eqs. (13)–(15), are needed.

As a consequence, the efficiencies of the heat sources are influenced. The key system performance indexes such as the annual usage of the peak boiler are summarized in Table 8. In the DHWT system, the recovered waste heat from industrial processes is reduced and the peak boiler usage is therefore increased. Indeed, the DHWT system has even higher peak boiler usage than the REF system. Thus, unlike in the peak scenario, the cost-saving rate of the DHWT is lower than the CWT and BTM systems.

5.3. The influence of substation design

The three heat source scenarios were also simulated with the triple-pipes design to identify the influence of this alternative design on the TES performances. Fig. 15 shows the comparisons of cost-savings for different substation designs. The results indicate that the benefit of the DHWT is heavily influenced by the substation design while the benefits of the CWT and the BTM are only slightly changed. With the triple-pipes design, there is no bypass loss and the cost-savings of the DHWT can be even negative due to the reasons such as the high heat loss, explained in
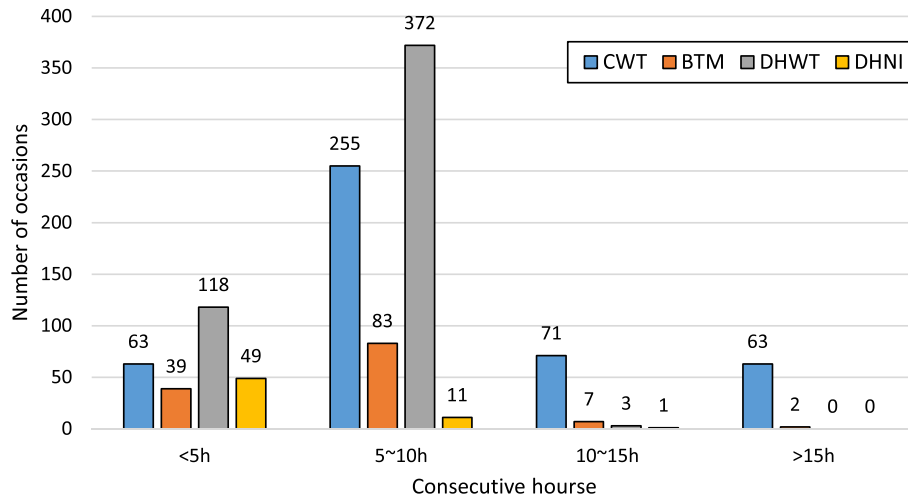
Fig. 13. Number of occasions for different TES options when the state-of-charges are higher than 70% of their design values.
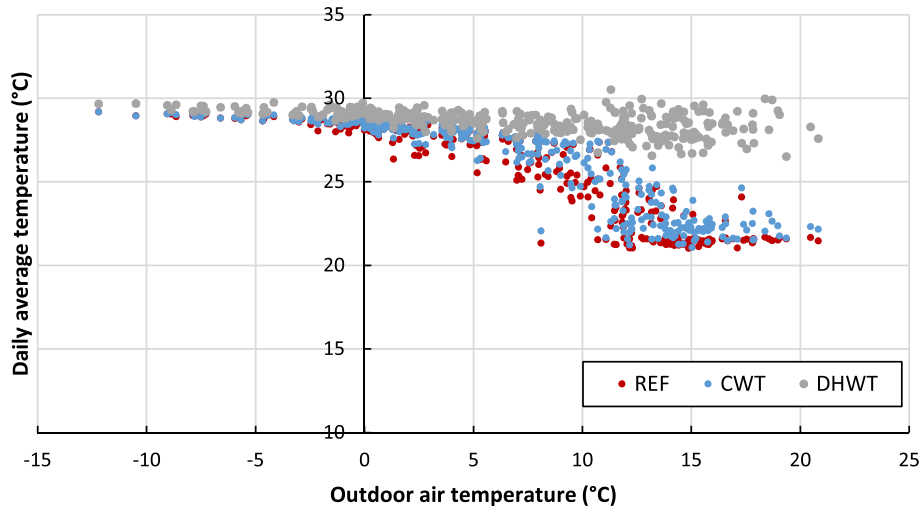

Fig. 14. Daily average return water temperature of the REF, CWT, and DHWT systems in the IWH scenario.

Table 8
Average return water temperature, peak boiler usage and operation costs of the case system in IWH scenario.

Scenarios	Return temperature (°C)	IWH usage (MWh)	Peak boiler usage (MWh)	Cost (SEK)	Annual cost-saving rate (%)
REF	25.8	1795	276	581,688	–
CWT	26.2	1810	264	−7340	1.26%
BTM	25.9	1818	255	−10,426	1.79%
DHWT	28.6	1696	294	−3363	0.58%
DHNI	25.8	1747	327	26,631	−4.58%

above sections. Thus, in the future LTDH systems, the choice between the DHWT design and the triple-pipes design is required. The heat losses in the systems with the triple-pipes design are presented in Table 9, based on the peak source scenario. Compared to the heat losses presented in Fig. 11, the network loss is slightly increased due to the losses from the third pipes. However, overall heat losses are reduced.

5.4. The influence of SH demand

The annual cost-savings of the investigated systems with the future

low-energy building stock are presented in Fig. 16. Due to the infeasible usage of DHNI as proved in the above sections, the results for the DHNI are not presented. From the current building stock to the future low-energy buildings, the cost-saving rates for all systems are increased to some levels. However, for the system with BTM, the cost-saving rate is only slightly changed because there is less storage potential from the better insulated buildings. The use of BTM is directly influenced by the space heating demand. In the current building stock, there are totally 150 days, where the BTM is actively used. In the future low-energy building stock, since the SH demand is greatly reduced, BTM is only used in 100 days. Thus, the number of full-load discharge cycles in the low-energy building stock scenario is approximately half of the number in current scenario, as shown in Fig. 17.

The system with the DHWT has the largest difference between the two building stock scenarios. This is also explained by the bypass losses. In the future low-energy building stock, due to the reduced demand for SH, the bypass loss becomes higher in the whole system, as shown in Fig. 9. Indeed, the annual bypass loss is 11.6 kWh/m², which is around 18% of the total heat supply. The benefit of reduced bypass loss can even to some extent offset the extra cost related to the DHWT in the IWH scenario, with the annual cost-saving rate reached 6.6% in the low-energy building stock. Thus, the original DHWT design has more benefits while the DHWT with the triple-pipes design has basically negative cost-savings. Compared to the peak scenario, the influence of bypass loss
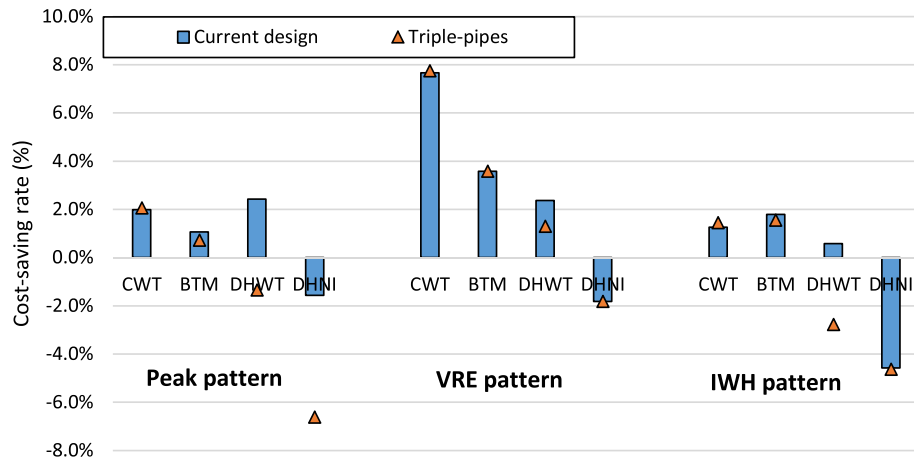
Fig. 15. Annual cost-savings for the systems with the current substation design and the triple-pipes design.

Table 9
Heat losses in the systems with the triple-pipes design, under peak scenario.

Cases	Network loss (kWh/m²)	TES loss (kWh/m²)	Total (kWh/m²)	Loss rate (%)
REF	7.7	0.0	7.7	7.8%
CWT	7.6	0.2	7.9	8.0%
BTM	7.6	0.5	8.1	8.2%
DHWT	6.6	2.3	8.9	8.9%
DHNI	10.3	0.0	10.3	9.8%

Table A1
Linear heat loss coefficient and network construction cost [48].

Nominal diameter	Linear heat loss coefficient (W/m·K)		Cost
	Supply	Return	(SEK/m)
DN12	0.095	0.040	1200
DN16	0.100	0.045	1500
DN20	0.105	0.054	1769
DN25	0.110	0.071	1909
DN32	0.115	0.127	2002
DN40	0.120	0.140	2149
DN50	0.125	0.143	2416
DN65	0.130	0.150	2608
DN80	0.135	0.160	2958
DN100	0.140	0.170	3189
DN125	0.145	0.180	3523
DN150	0.150	0.190	4082

is less significant in the VRE scenario, as illustrated in the Section 5.2.

Comparing the four TES technologies, the use of CWT is most favourable in the VRE scenario, with an annual cost-saving rate of 15.1% in the future low-energy buildings.

5.5. Sensitivity analysis

In the above analysis, a 0.5 K temperature deviation is considered for using the BTM, as a conservative evaluation of the residents' acceptance for temperature changes, according to the field measurement [34]. However, the storage potential can still be further increased by allowing larger temperature deviations. Thus, three scenarios, with deviations of 1 K, 1.5 K and 2 K, are modelled and compared, as shown in Fig. 18.

The benefits of using the BTM is not linearly related to the temperature deviations. Little benefits are found from the increased use of the BTM in the peak heat source scenario since the peak load is mainly induced by the instantaneous DHW demand instead of the SH demand. A temperature increase of more than 1 K can even lead to negative impact due to the increased space heating demand. In contrary, in the VRE

scenario, the larger temperature deviation increases the storage potential and, thus, increases the VRE integration and enlarges the benefits. However, similar as the case in the peak scenario, the benefit of the BTM only increases slightly when the temperature deviation is larger than 1 K. Therefore, in the investigated cases, a suitable choice of the temperature deviation level would be 1 K, to maximize the benefits while maintaining an acceptable thermal comfort range. As for the use of the DHWT, a prominent limitation is the high thermal loss due to a poor insulation. However, as the technology develops, there is possibility of a cheaper and space-saving thermal insulation, with less heat loss factor, for the small-scale DHWTs in the future. Thus, the sensitivity of the heat loss factors is analysed on different scenarios and shown in Fig. 19. It is apparent that the benefit of the DHWT becomes larger when the heat loss factor is reduced. As explained in Section 5.1, since the major benefit of the DHWT comes from the reduction of bypass loss, the DHWT has similar cost-saving rates in the peak scenario and VRE scenario. Compared to the CWT, the DHWT still has less potential for integrating the VRE, even though the heat losses can be reduced by improved thermal insulations.

6. Discussion

6.1. Applicability of TES technologies in the future

Based on the simulated results from all the scenarios in this study, a performance map of TES technologies under the future DH changes is shown in Fig. 20. Possible transitions from the current heating system to the future heating system can be classified into changes in three parts as explained in Section 4, of which the changes in the end-use demand side and the changes in the heat source supply side are considered as two main variables during the analysis. The central idea is that the future design and usage of TES technologies should be highly in accordance with the characteristics of the future energy systems. Several transitions for the TES applications are summarized as follows:

①: Major changes take place in the end-use buildings. This transition is likely to happen in middle and large cities where the VRE resource is scarce. As the renovation works are conducted in the buildings, changes in the substations are also needed. As discussed in Section 5.3, both DHWT design and the triple-pipes design can reduce the unnecessary bypass loss and increase system efficiency, but only one option is enough. The former design requires more strict control of the water temperature, and the latter design requires renovations of the pipe system.

②: Major changes take place in the heat sources, with increased VRE generations. This transition refers to the DH systems where heat and power networks are connected through heat pumps or CHP plants.
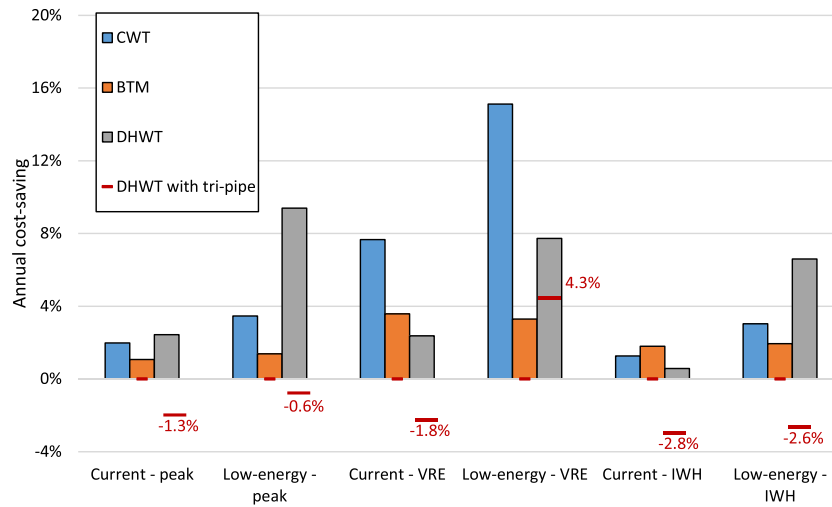
Fig. 16. Annual cost-savings under different heat source scenarios and building stock scenarios.
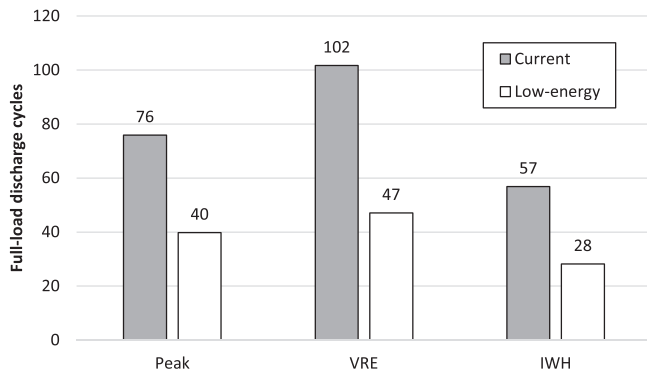

Fig. 17. Full-load discharge cycles of the BTM in current and low-energy building stocks.

Comparing the TES technologies, central and compact unit with small heat loss rate and high control flexibility, such as the CWT in this study, can better balance the supply and demand and, thus, has the largest potential for applications.

③: The share of renewable energy is also increased in this transition but, unlike transition ②, the DH systems have less interactions with the

power system. Possible heating sources include the direct use of industrial waste heat and biomass boilers. The prospective benefits for TES technologies are mainly related to the peak load reduction and smooth system operation, which can be lower than the benefits in transitions ① and ②. As shown in Fig. 16, the differences between TES options are relatively small.

④: A direct transition towards the future LTDH system, which is likely to happen in newly built districts with good building thermal insulation and abundant VRE production. A combination of the supply side central TES option and the demand side measures is required.

6.2. Limitations

The results of this study are based on a small-scale LTDH system in the case residential community, with 165 SFHs. This case represents the typical small community in the suburban or rural area in the Northern Europe, with a unidirectional centralized heat supply system. However, there are growing interest for multi-sources de-centralized heating systems, including both the unidirectional type and bi-directional type. As the space heating demand goes down in the future, the conventional centralized district heating system will become less feasible from both the economic and technical aspects. These challenges call for flexible measures to balance the energy supply in the demand side.

Therefore, the future research focuses will be put on the optimal
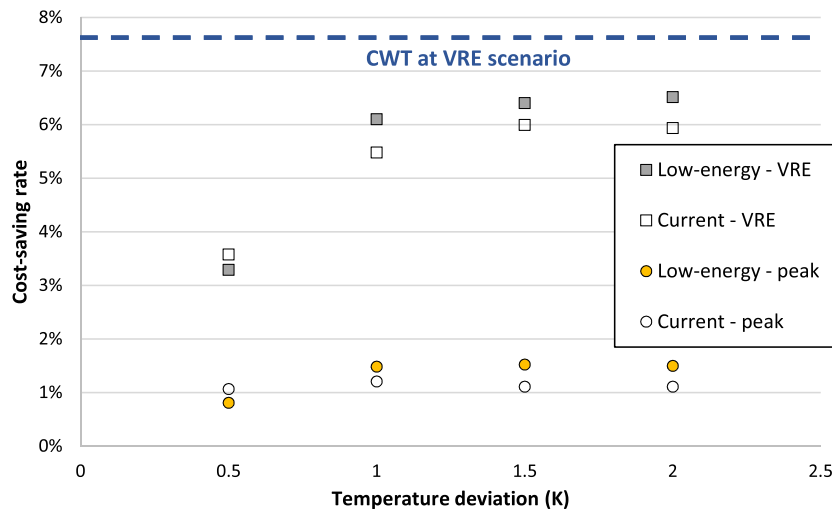

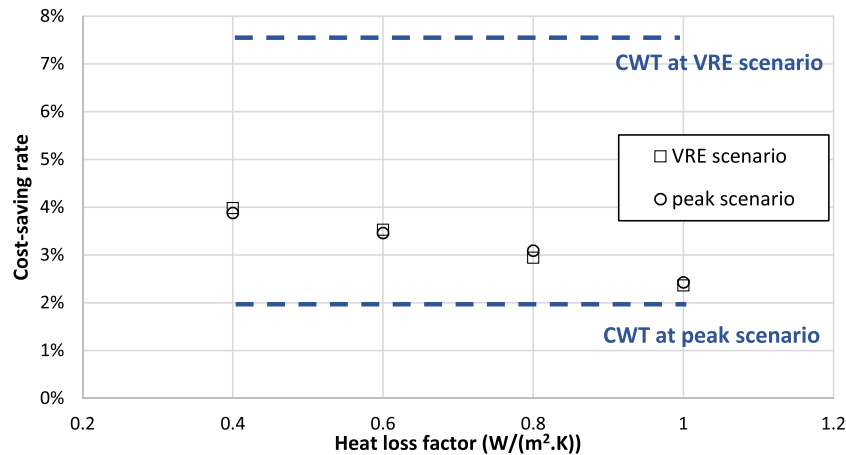**Fig. 18.** Sensitivity analysis of the temperature deviations for using the BTM.

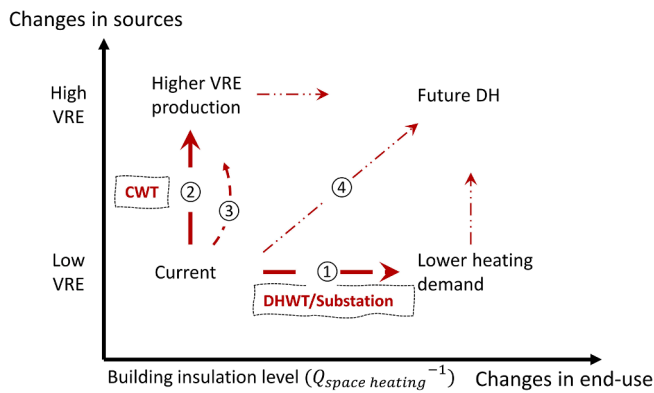**Fig. 19.** Sensitivity analysis of the heat loss factors of the DHWT.

Fig. 20. Performance map of the TES technologies under the future changes of the DH systems.

design and operation of de-centralized heating systems. Besides, in the multi-sources DH systems, the costs related to the start-ups and the ramping of heat sources are important parts in the total operation cost and thereby become one of the main incentives to install TES units [37]. Considering the above aspects, the applications of TES technologies shall be further examined. Besides, since the temperature levels of the whole system will be reduced, there are less potentials for sensible TES units, while other types of storage technologies, such as latent TES utilizing the phase-change materials, could have more potentials. Together with the results in this study, a better understanding about the roles of TES technologies in the future can be acquired.

As is mentioned in the above Section 6.1, the analysis indicators used in this study are focusing on the TES unit itself, such as the discharge cycles and cost-saving rate. However, TES units also has important influences on the sizes of the network and heating source, as indicated in [59]. The benefits of reduced investments in the pipes and heat sources are not considered in this study.

7. Conclusion

With the aim of evaluating the applicability of TES technologies in the future LTDH systems, a case LTDH system was simulated and compared under various representative scenarios of the future changes, including the changes in the source side, network side, and the end-use demand side. For each scenario, this study compared the operating performances and cost-savings of four typical short-term TES technologies. Considering the growing need in the transitions from the current energy systems to the future sustainable and smart energy systems,

conclusions on how the specific TES technologies are adapted to the future systems are summarized as follows:

1) The results show that the four TES technologies can balance the heat supply and demand to some extent. Besides the benefits of load shifting, the use of distributed domestic hot water tanks (DHWTs) can also reduce the bypass loss in the substations and, thereby, has the largest cost-savings in the current peak source scenario. It is proved that the triple-pipes design in the substation can also solve this issue, implying a choice between the two substation designs.
2) Due to the relatively small heat loss and the control flexibility, the central water tank (CWT) is able to store heat for longer period than the other TES technologies and is thus suitable for integrating the VRE in the future. In contrary, since the energy price is basically low during the summer when the VRE is abundant, the previous benefits associated with the DHWT for reducing the bypass loss is less significant.
3) As the space heating demand goes down in the future, there is less storage potential from the use of building thermal mass (BTM). Since the space-heating period is reduced, the BTM is only used for less than 100 days in the future low-energy buildings. However, the bypass loss becomes even more prominent during the non-space-heating period, calling for measures in the demand side.
4) The use of district heating network inertia (DHNI) as storage unit is proved to be infeasible in all scenarios based on the case LTDH systems. The main reason is that the heat source efficiency is significantly reduced by raising the supply water temperature. Besides, since the storage capacity of the networks in small-scale systems is as small as less than 1% of the daily heat load, the proposed benefits cannot even offset the increased network heat losses.

Finally, based on the results from all analysed scenarios, it is pointed out that the designs and applications of TES technologies shall be designed in accordance with the characteristics of the future LTDH systems to avoid under-estimations or over-estimations of the roles of TES technologies.

CRediT authorship contribution statement

Yichi Zhang: Methodology, Validation, Investigation, Formal analysis, Writing - original draft. **Pär Johansson:** Conceptualization, Writing - review & editing, Supervision. **Angela Sasic Kalagasidis:** Conceptualization, Resources, Writing - review & editing, Supervision.

Declaration of Competing Interest

The authors declare that they have no known competing financial

interests or personal relationships that could have appeared to influence the work reported in this paper.

Acknowledgement

This work was supported by the Swedish Research Council for Environment, Agricultural Sciences and Spatial Planning (FORMAS) [Grant No. 2018-01228].

References

[1] Lund H. Renewable energy strategies for sustainable development. Energy 2007;32 (6):912–9. https://doi.org/10.1016/j.energy.2006.10.017.

[2] Mathiesen BV, Lund H, Connolly D, Wenzel H, Østergaard PA, Möller B, et al. Smart Energy Systems for coherent 100% renewable energy and transport solutions. Appl Energy 2015;145:139–54. https://doi.org/10.1016/j.apenergy.2015.01.075.

[3] Intergovernmental Panel on Climate Change, editor. Summary for Policymakers. Clim. Chang. 2013 – Phys. Sci. Basis Work. Gr. I Contrib. to Fifth Assess. Rep. Intergov. Panel Clim. Chang., Cambridge: Cambridge University Press; 2014, p. 1–30. https://doi.org/DOI: 10.1017/CBO9781107415324.004.

[4] Lund H, Werner S, Wiltshire R, Svendsen S, Thorsen JE, Hvelplund F, et al. 4th Generation District Heating (4GDH) Integrating smart thermal grids into future sustainable energy systems. Energy 2014;68:1–11. https://doi.org/10.1016/j.energy.2014.02.089.

[5] Lund H, Østergaard PA, Chang M, Werner S, Svendsen S, Sorknæs P, et al. The status of 4th generation district heating: Research and results. Energy 2018;164: 147–59. https://doi.org/10.1016/j.energy.2018.08.206.

[6] Connolly D, Lund H, Mathiesen BV, Werner S, Möller B, Persson U, et al. Heat roadmap Europe: Combining district heating with heat savings to decarbonise the EU energy system. Energy Policy 2014;65:475–89. https://doi.org/10.1016/j.enpol.2013.10.035.

[7] Lund H, Østergaard PA, Connolly D, Mathiesen BV. Smart energy and smart energy systems. Energy 2017;137:556–65. https://doi.org/10.1016/j.energy.2017.05.123.

[8] Guelpa E, Verda V. Thermal energy storage in district heating and cooling systems: A review. Appl Energy 2019;252:113474. https://doi.org/10.1016/j.apenergy.2019.113474.

[9] Hewitt NJ. Heat pumps and energy storage – The challenges of implementation. Appl Energy 2012;89(1):37–44. https://doi.org/10.1016/j.apenergy.2010.12.028.

[10] David A, Mathiesen BV, Averfalk H, Werner S, Lund H. Heat Roadmap Europe: Large-scale electric heat pumps in district heating systems. Energies 2017;10:1–18. https://doi.org/10.3390/en10040578.

[11] Lund H. Renewable heating strategies and their consequences for storage and grid infrastructures comparing a smart grid to a smart energy systems approach. Energy 2018;151:94–102. https://doi.org/10.1016/j.energy.2018.03.010.

[12] Lund H, Østergaard PA, Connolly D, Mathiesen BV. Energy storage and smart energy systems. Energy 2017;137:556–65. https://doi.org/10.1016/j.energy.2017.05.123.

[13] Salpakari J, Mikkola J, Lund PD. Improved flexibility with large-scale variable renewable power in cities through optimal demand side management and power-to-heat conversion. Energy Convers Manag 2016;126:649–61. https://doi.org/10.1016/j.enconman.2016.08.041.

[14] Child M, Bogdanov D, Breyer C. The role of storage technologies for the transition to a 100% renewable energy system in Europe. Energy Procedia 2018;155:44–60. https://doi.org/10.1016/j.egypro.2018.11.067.

[15] Persson U, Möller B, Werner S. Heat Roadmap Europe: Identifying strategic heat synergy regions. Energy Policy 2014;74:663–81. https://doi.org/10.1016/j.enpol.2014.07.015.

[16] Gadd H, Werner S. Thermal energy storage systems for district heating and cooling. Woodhead Publ Ltd 2015. https://doi.org/10.1533/9781782420965.4.467.

[17] Hennessy J, Li H, Wallin F, Thorin E. Flexibility in thermal grids: A review of short-term storage in district heating distribution networks. Energy Procedia 2019;158: 2430–4. https://doi.org/10.1016/j.egypro.2019.01.302.

[18] Enescu D, Chicco G, Porumb R, Seritan G. Thermal energy storage for grid applications: Current status and emerging trends. Energies 2020;13. https://doi.org/10.3390/en13020340.

[19] Zheng W, Hennessy JJ, Li H. Reducing renewable power curtailment and CO2 emissions in China through district heating storage. Wiley Interdiscip Rev Energy Environ 2020;9:1–11. https://doi.org/10.1002/wene.361.

[20] Averfalk H, Werner S. Novel low temperature heat distribution technology. Energy 2018;145:526–39. https://doi.org/10.1016/j.energy.2017.12.157.

[21] Schmidt D, Kallert A, Blesl M, Svendsen S, Li H, Nord N, et al. Low temperature district heating for future energy systems. Energy Procedia 2017;116:26–38. https://doi.org/10.1016/j.egypro.2017.05.052.

[22] Yang X, Li H, Svendsen S. Energy, economy and exergy evaluations of the solutions for supplying domestic hot water from low-temperature district heating in Denmark. Energy Convers Manag 2016;122:142–52. https://doi.org/10.1016/j.enconman.2016.05.057.

[23] Schmidt D, Kallert A, Blesl M, Li H, Svendsen S, Nord N, et al. Annex TS1 Low Temperature District Heating for Future Energy Systems - Final report - Future low temperature district heating design guidebook. 2017.

[24] Dalla Rosa A, Li H, Svendsen S. Method for optimal design of pipes for low-energy district heating, with focus on heat losses. Energy 2011;36(5):2407–18. https://doi.org/10.1016/j.energy.2011.01.024.

[25] Yang X. Supply of domestic hot Water at comfortable temperatures by low-temperature district heating without risk of Legionella. 2016.

[26] Nielsen JE. IEA-SHC Task 45: Large solar heating/cooling systems, seasonal storage, heat pumps. Energy Procedia 2012;30:849–55. https://doi.org/10.1016/j.egypro.2012.11.096.

[27] Verda V, Colella F. Primary energy savings through thermal storage in district heating networks. Energy 2011;36(7):4278–86. https://doi.org/10.1016/j.energy.2011.04.015.

[28] Eriksson R. Heat storages in Swedish district heating systems. An analysis of the installed thermal energy storage capacity 2016:40.

[29] de Wit J. Heat Storages for CHP Optimisation. PowerGen Eur 2007;2007:1–18.

[30] Li H, Svendsen S. Energy and exergy analysis of low temperature district heating network. Energy 2012;45(1):237–46. https://doi.org/10.1016/j.energy.2012.03.056.

[31] Yang X, Li H, Svendsen S. Evaluations of different domestic hot water preparing methods with ultra-low-temperature district heating. Energy 2016;109:248–59. https://doi.org/10.1016/j.energy.2016.04.109.

[32] Tol Hİ, Svendsen S. Improving the dimensioning of piping networks and network layouts in low-energy district heating systems connected to low-energy buildings: A case study in Roskilde. Denmark. Energy 2012;38(1):276–90. https://doi.org/10.1016/j.energy.2011.12.002.

[33] Hedegaard K, Mathiesen BV, Lund H, Heiselberg P. Wind power integration using individual heat pumps – Analysis of different heat storage options. Energy 2012;47 (1):284–93. https://doi.org/10.1016/j.energy.2012.09.030.

[34] Kensby J, Trüschel A, Dalenbäck JO. Potential of residential buildings as thermal energy storage in district heating systems – Results from a pilot test. Appl Energy 2015;137:773–81. https://doi.org/10.1016/j.apenergy.2014.07.026.

[35] Gu W, Wang J, Lu S, Luo Z, Wu C. Optimal operation for integrated energy system considering thermal inertia of district heating network and buildings. Appl Energy 2017;199:234–46. https://doi.org/10.1016/j.apenergy.2017.05.004.

[36] Guelpa E, Barbero G, Sciacovelli A, Verda V. Peak-shaving in district heating systems through optimal management of the thermal request of buildings. Energy 2017;137:706–14. https://doi.org/10.1016/j.energy.2017.06.107.

[37] Romanchenko D, Kensby J, Odenberger M, Johnsson F. Thermal energy storage in district heating: Centralised storage vs. storage in thermal inertia of buildings. Energy Convers Manag 2018;162:26–38. https://doi.org/10.1016/j.enconman.2018.01.068.

[38] Vanhoudt D, Claessens BJ, Salenbien R, Desmedt J. An active control strategy for district heating networks and the effect of different thermal energy storage configurations. Energy Build 2018;158:1317–27. https://doi.org/10.1016/j.enbuild.2017.11.018.

[39] Werner S. District heating and cooling 2013.

[40] Zheng J, Zhou Z, Zhao J, Wang J. Integrated heat and power dispatch truly utilizing thermal inertia of district heating network for wind power integration. Appl Energy 2018;211:865–74. https://doi.org/10.1016/j.apenergy.2017.11.080.

[41] Wang J, Zhou Z, Zhao J, Zheng J. Improving wind power integration by a novel short-term dispatch model based on free heat storage and exhaust heat recycling. Energy 2018;160:940–53. https://doi.org/10.1016/j.energy.2018.07.018.

[42] Li Z, Wu W, Shahidehpour M, Wang J, Zhang B. Combined heat and power dispatch considering pipeline energy storage of district heating network. IEEE Trans Sustain Energy 2016;7(1):12–22. https://doi.org/10.1109/TSTE.2015.2467383.

[43] Benonysson A, Bøhm B, Ravn HF. Operational optimization in a district heating system. Energy Convers Manag 1995;36(5):297–314.

[44] Zhao H. Analysis, modelling and operational optimization of district heating systems, 1995.

[45] de Normalización CE. EN ISO 13790: Energy Performance of Buildings: Calculation of Energy Use for Space Heating and Cooling (ISO 2008;13790::2008).. .

[46] Jordan U, Vajen K. Realistic domestic hot-water profiles in different time scales. Rep Sol Heat Cool Progr Int Energy Agency (IEA-SHC)Task 2001;26:1–18.

[47] SFS-EN 15316-3-1. Heating systems in buildings — Method for calculation of system energy requirements and system efficiencies — Part 3-1 Domestic hot water systems , characterisation of needs (tapping requirements) 2006:1–20.

[48] Best I, Orozaliev J, Vajen K. Economic comparison of low-temperature and ultra-low-temperature district heating for new building developments with low heat demand densities in Germany. Int J Sustain Energy Plan Manag 2018;16:45–60. https://doi.org/10.5278/ijsepm.2018.16.4.

[49] Guelpa E, Sciacovelli A, Verda V. Thermo-fluid dynamic model of large district heating networks for the analysis of primary energy savings. Energy 2019;184: 34–44. https://doi.org/10.1016/j.energy.2017.07.177.

[50] Alimohammadisagvand B, Jokisalo J, Kilpeläinen S, Ali M, Sirén K. Cost-optimal thermal energy storage system for a residential building with heat pump heating and demand response control. Appl Energy 2016;174:275–87. https://doi.org/10.1016/j.apenergy.2016.04.013.

[51] Renaldi R, Kiprakis A, Friedrich D. An optimisation framework for thermal energy storage integration in a residential heat pump heating system. Appl Energy 2017; 186:520–9. https://doi.org/10.1016/j.apenergy.2016.02.067.

[52] Guadalfajara M, Lozano M, Serra L. Analysis of Large Thermal Energy Storage for Solar District Heating. Eurotherm Semin #99 Adv Therm Energy Storage 2014: 1–10. https://doi.org/10.13140/2.1.3857.6008.

[53] Cruickshank CA, Harrison SJ. Heat loss characteristics for a typical solar domestic hot water storage. Energy Build 2010;42(10):1703–10. https://doi.org/10.1016/j.enbuild.2010.04.013.

[54] Maivel M, Kurnitski J. Heating system return temperature effect on heat pump performance. Energy Build 2015;94:71–9. https://doi.org/10.1016/j.enbuild.2015.02.048.

[55] NordPool Group. NordPool, the leading power market in Europe n.d. https://www.nordpoolgroup.com/ (accessed February 16, 2020).

[56] AE Solar. AE Solar Product list 2020. https://ae-solar.com/products-list/ (accessed December 25, 2020).

[57] Commission JRCE. Photovoltaic geographical information system-interactive maps 2014.

[58] Averfalk H, Werner S. Economic benefits of fourth generation district heating. Energy 2020;193:116727. https://doi.org/10.1016/j.energy.2019.116727.

[59] Jebamalai JM, Marlein K, Laverge J. Influence of centralized and distributed thermal energy storage on district heating network design. Energy 2020;202:117689. https://doi.org/10.1016/j.energy.2020.117689.